REPORT DOCUMENTATION PAGE

Form Approved
OMB No. 0704-0188

PLEASE DO NOT RETURN YOUR FORM TO THE ABOVE ADDRESS.

1. REPORT DATE *(DD-MM-YYYY)*	2. REPORT TYPE	3. DATES COVERED *(From - To)*
06-16-08	Interim	December 13, 2007 to June 13, 2008

4. TITLE AND SUBTITLE

Effects of Subzero Temperatures and Seawater Immersion on Damage Initiation and Growth in Sandwich Composites.

5a. CONTRACT NUMBER

N/A

5b. GRANT NUMBER

N00014-07-1-0418

5c. PROGRAM ELEMENT NUMBER

N/A

6. AUTHOR(S)

Davidson, Barry, D.

5d. PROJECT NUMBER

N/A

5e. TASK NUMBER

N/A

5f. WORK UNIT NUMBER

N/A

7. PERFORMING ORGANIZATION NAME(S) AND ADDRESS(ES)

Syracuse University
Department of Mechanical and Aerospace Engineering
149 Link Hall
Syracuse, New York 13244

8. PERFORMING ORGANIZATION REPORT NUMBER

N/A

9. SPONSORING/MONITORING AGENCY NAME(S) AND ADDRESS(ES)

Yapa D. S. Rajapakse
Office of Naval Research
875 North Randolph Street
Arlington, VA 22203-1995

10. SPONSOR/MONITOR'S ACRONYM(S)

N/A

11. SPONSOR/MONITOR'S REPORT NUMBER(S)

N/A

12. DISTRIBUTION/AVAILABILITY STATEMENT

Approved for public release; distribution unlimited.

13. SUPPLEMENTARY NOTES

N/A

14. ABSTRACT

Progress during the past six months is described. Efforts during this period have focused on (1) immersion studies of core and sandwich laminates, (2) the effects of environment on impact damage and fatigue response, and (3) debonding test development and toughness assessments. Ongoing studies in the first area indicate that there is no appreciable difference in the sea water absorption rate or saturation level for samples immersed at room temperature versus immersion at 0°C. In the second focus area, approximately 50% of the proposed test program has been completed, allowing a number of preliminary conclusions to be drawn about the effects of temperature, sea water saturation, and damage on the static strength, stiffness, fatigue life and fatigue strength of sandwich laminates. In the third focus area, work on validating a new, highly accurate debonding test is nearly complete. Specimens have also been manufactured and sea water conditioned in preparation for subsequent use of this test method to study the effect of temperature and sea water immersion on toughness.

15. SUBJECT TERMS

Sandwich, composites, freezing, temperature, seawater, fracture, impact, fatigue, dynamic

16. SECURITY CLASSIFICATION OF:			17. LIMITATION OF ABSTRACT	18. NUMBER OF PAGES	19a. NAME OF RESPONSIBLE PERSON
a. REPORT	b. ABSTRACT	c. THIS PAGE			Barry D. Davidson
U	U	U	UU	8	19b. TELEPHONE NUMBER *(Include area code)* 315-443-4201

Effects of Subzero Temperatures and Seawater Immersion on Damage Initiation and Growth in Sandwich Composites

Interim Report for the period December 13, 2007 –June 13, 2008

Barry D. Davidson

June 16, 2008

Executive Summary

Progress during the past six months is described on the project "Effects of Subzero Temperatures and Seawater Immersion on Damage Initiation and Growth in Sandwich Composites." Efforts during this period have focused on (1) immersion studies of core and sandwich laminates, (2) the effects of environment on impact damage and fatigue response, and (3) debonding test development and toughness assessments. Ongoing studies in the first area indicate that there is no appreciable difference in the sea water absorption rate or saturation level for samples immersed at room temperature versus immersion at 0°C. In the second focus area, approximately 50% of the proposed test program has been completed, allowing a number of preliminary conclusions to be drawn about the effects of temperature, sea water saturation, and damage on the static strength, stiffness, fatigue life and fatigue strength of sandwich laminates. In the third focus area, work on validating a new, highly accurate debonding test is nearly complete. Specimens have also been manufactured and sea water conditioned in preparation for subsequent use of this test method to study the effect of temperature and sea water immersion on toughness.

Introduction

As described above, research efforts have focused on (1) immersion studies of core and sandwich laminates, (2) the effects of environment on impact damage and fatigue response, and (3) debonding test development and toughness assessments. Details on these efforts, their current status, and the plans for completion are provided in the ensuing sections. This is followed by an updated Gantt chart showing the projected schedule to completion for the entire research effort.

Immersion Studies

The follow-up core and sandwich immersion studies described in the last interim report were initiated during the current period of work. Surprisingly, the previous results, which showed a more rapid initial moisture absorption rate at 0°C than at room temperature (RT) could not be duplicated. Rather, the new results showed essentially no difference in sea water absorption rates or final saturation levels at the two temperatures. To understand the reason for the discrepancies, additional studies were performed, including the effect of specimen size and cutting method. That is, in the initial study, some core samples were cut with a table saw and some were cut with a diamond saw, whereas in the follow-up study a band saw was used for all specimens. The effects of these three cutting methods were therefore studied over a range of specimen sizes. In all, 5 separate batches of samples were studied. Because of the long-term nature of these studies, data is still being gathered and analyzed. However, current indications are that all of the follow-up studies show no significant effect of cutting method or temperature (for RT versus 0°C) on the rate of sea water absorption or on the long-term saturation level. The reason for the anomalous

results from the first batch is still unknown. However, the important finding – which is consistent among all studies – is that the long-term saturation level is unaffected.

In addition to the above, a study was also initiated to evaluate the effects of sea water "sloshing" on moisture absorption rates and saturation levels. To this end, selected containers holding the sea water immersed specimens were placed on a low frequency oscillating shaker table. This study is also still in progress. However, initial indications are that moisture absorption rates are essentially the same, or perhaps even a bit slower, on the shaker table as compared to static immersion.

Preliminary Conclusions and Next Steps

The preliminary conclusions from this portion of the study are as follows:

- Sea water absorption rates and final saturation levels in PVC foam core specimens appear to be relatively unaffected by temperature differences in the range of 0° to 20°C. The reason for one batch of specimens that shows different results is still under investigation.
- Effects of water sloshing on sea water absorption rates or final saturation levels are still being investigated but are expected to be small.
- Room temperature immersion is concluded to be equally deleterious as immersion at 0°C for PVC foam core and PVC foam core sandwich structures.

We have moved forward with the decision from the last interim report to *perform all moisture conditioning of the specimens to be used in this research at RT* and, as will be described subsequently, many specimens have already been fully saturated for testing. A limited amount of work to complete the immersion studies remains to be performed and includes the following steps:

- Complete the current sea water absorption studies to complete saturation to validate (or modify as needed) the above preliminary conclusions.
- Examine specimens after long immersion times (at both temperatures) where saturation has definitively been reached. Freeze these fully saturated specimens and compare the results to those already obtained.
- Examine the effects of a second saturation and freeze cycle, i.e., for specimens that have been saturated, frozen, re-saturated, and then frozen a second time.
- Document results of significance in the form of an archival journal publication.

Bending Test Program

Determination of Test Geometry, Environment and Impact Energy

As described in the last interim report, it was found that 12.7mm thick Diab H100 core was necessary in order to obtain core shear failures. This core was received and a sandwich panel with 6 ply glass/vinylester face sheets was manufactured. Specimens were cut and tested in four-point bending with a load pad spanning the inner loading heads. Static and fatigue tests were performed. Local face sheet crushing was observed in the static tests, and a combined face sheet

crushing, face sheet tension and core shear failure mode was observed in the fatigue tests. For these reasons, specimens with 8 ply thick face sheets were then manufactured. Exploratory tests at room temperature showed that the desired core shear failure mode occurred for both static and fatigue loadings.

Having established that the specimen geometry was acceptable at room temperature, exploratory fatigue tests were then conducted at -40°C, for which core shear or combined face sheet tension and core shear failures were observed. However, due to the heat generated from the fatigue test, it was found that the Syracuse University Composite Materials Laboratory (SU-CML) low temperature chamber could not maintain a constant -40°C temperature. For this reason, the test temperature was changed to -20°C, for which additional exploratory tests showed that a constant temperature could be maintained. To verify the temperature distribution within the specimen, 4 "double-width" specimens were outfitted with 4 thermocouples each. The 4 thermocouples were distributed lengthwise, and all were more than 25mm from the specimen's ends. All thermocouples were located 13mm from the free edge in the width direction. Two thermocouples were located at the thickness mid-plane, one was at the upper face sheet-to-core interface, and one was located at the at the lower face sheet-to-core interface. Temperature uniformity tests were then conducted, for which it was established that the temperature at all points within the specimen stayed within 2°C of the desired set-point for the entire test. Cool-down tests were also conducted, for which it was established that 60 minutes in the low temperature chamber was required for the specimen to stabilize at the desired temperature. To be conservative, all subsequent tests therefore allowed a 90 minute period within the freezer before initiating the test.

Following the above, a series of exploratory impact tests were conducted. Impact energies between 6 and 12J were considered. Impacts of 10J were observed to produce damage that was observable, but that did not produce "excessive" permanent deformation. That is, it was believed to be representative of worst-case damage that might go unrepaired in a practical structure. Additional exploratory tests were then conducted on seawater saturated specimens, for which the same conclusions were obtained. Therefore, 10J was chosen as the impact energy for this test program.

Detailed Description of Test Geometry and Impact Fixture

Figure 1 presents a schematic of the final test geometry. All test specimens were nominally 305mm long x 25.4mm wide and were tested in bending with an outer span length of 279.4mm. Each loading head has a 25mm diameter cylindrical loading surface. For impact damaged specimens, impacts were always introduced so that they were in the middle of the half-span, i.e., mid-way between the loading and support head on one side. Impact-damaged specimens were always tested so that the impacted region was on the upper, compressive side of the specimen during the test.

Figure 2 presents a photograph of the SU-CML low temperature chamber, and Figure 3 presents a photograph of the bending fixture that was taken through one of the side windows. The load pad arrangement shown in Figure 3 was chosen to eliminate local face sheet crushing yet still obtain the desired mode of crack growth during failure. The load pad consists of two parts: the first is a 54.2mm long x 32.1mm wide x 6.6mm thick piece of aluminum that spans the inner loading heads. The second part consists of a 65.4mm long x 35.2mm wide x 3.6mm thick piece of rubber that is placed between the aluminum load pad and the specimen.

The impact fixture is shown schematically in Figure 4, and a photograph of the fixture is presented in Figure 5. This fixture will accommodate specimens up to 75mm wide. An impactor with a 25mm diameter, cylindrically shaped impact head is dropped through a guide tube to impact the specimen at the desired location. A capture device captures the impactor upon its first rebound, such that only a single impact occurs on any given drop. Boundary conditions can be fully supported along the entire base as depicted in Figure 4, or the panel can be simply supported at each end. Toggle clamps are used at the four corners of the panel to hold it in place. The point of impact can be chosen by the user, such that the center of the impact damage will be in the correct location for subsequent testing. Two different impactors have been manufactured: one has a mass of 5.17kg and one has a mass of 2.67kg. Drop heights up to 800mm can be accommodated. For this study, the 2.67kg impactor was used with a drop height of 382mm to create the 10J impact energy. The panel was fully supported as shown in Figure 4.

Test Environments and Test Matrix

The original proposal for this research stated that fatigue experiments would be performed under the conditions of room temperature (RT) dry, –40°C dry, and sea water saturated held at –40°C. However, as described above, the low temperature (LT) environment was changed to -20°C to accommodate the SU-CML low temperature chamber limitations. Also, it was deemed important to add a RT test under sea water saturated conditions. Thus, a total of four test environments were defined. Further, under each environment, both undamaged and damaged tests were to be conducted. This leads to the following eight test conditions and their associated abbreviations:

LTDU – low temperature (-20°C) dry undamaged
LTDD – low temperature (-20°C) dry damaged

LTWU – low temperature (-20°C) wet (sea water saturated) undamaged
LTWD – low temperature (-20°C) wet (sea water saturated) damaged

RTDU – room temperature (20°C) dry undamaged
RTDD – room temperature (20°C) dry damaged

RTWU – room temperature (20°C) wet (sea water saturated) undamaged
RTWD – room temperature (20°C) wet (sea water saturated) damaged

As stated in the original proposal, three tests at each condition are being conducted, for a total of 24 fatigue tests. In addition to this, static tests to failure were deemed necessary in order to choose appropriate fatigue loads. Here, two tests per condition were first performed. A third static test to failure was added if a large difference in failure load was observed between the two tests at any condition. This resulted in a total of 22 static tests, and a few additional tests are still required. In order to maintain a consistent influence of the effects of panel-to-panel variation, at any condition, the specimens used for the static tests were taken from different panels. Similarly, the specimens used for the fatigue tests at any conditions are also being taken from different panels.

Specimen Manufacturing

The decision to use sandwich specimens with 8 ply face sheets was made in March 2008. At that time, we began to manufacture one panel per week. All sandwich panels were manufactured using BGF 7532 plain weave glass fabric and Dow Chemical's Derakane 411-350 vinyl ester resin. Each panel was 305mm long x 230mm wide and used a $[0/90/0/90]_s$ stacking sequence. Following manufacture, panels were cut into 25.4mm wide test specimens using a band saw. Thus, if there were no defects, each panel produces 8 specimens, and a minimum of 6 panels were therefore required to achieve the above test matrix. An additional 11 specimens were also used for exploratory testing, bringing the total number of panels required to 8. However, dry spots were found in a few panels – particularly in the first few manufactured, and some panels produced only 2-5 specimens. In those panels which produced only a few good specimens, these were used for the exploratory testing, whereas if a panel produced 4 or more good specimens they were included in the matrix of "good" specimens. As a result, a total of 13 panels were manufactured from which 11 specimens were used for exploratory testing and from which 59 good specimens remained. The average specimen thickness was 16.9mm, and varied from a minimum of 16.3mm to a maximum of 17.5mm with a standard deviation of 0.36mm.

In order to have specimens saturated in time for testing during the summer of 2008, approximately 50% of the specimens were immersed in sea water shortly after they were manufactured. In some cases, one-half of the specimens from a given plate were chosen for immersion, whereas in other cases all specimens from a given plate were chosen. These selections were based upon timing considerations (i.e., since dry specimens were immediately ready to test, one of the early panels was devoted to this and all specimens from a later panel were immersed) as well as the "balancing" of the entire test matrix to eliminate panel-to-panel variations as described above (i.e., only one test per condition from any one panel).

For those panels from which only half the specimens were sea water saturated, those selected constituted every-other-one from the cutting process, i.e., the specimens chosen were spread across the entire width of the original panel, rather than being chosen from just one side. In this way, any effects of spatially-varying properties within a given panel were minimized.

To achieve sea water saturation, the selected specimens were placed in plastic containers. "Control specimens" were also included with each new batch. The weight gain of these control specimens was monitored to assess saturation. Control specimens were 100mm long and of the same width and thickness as the test specimens. Once all test and control specimens were in place, the containers were filled to the top with sea water. Specially made polycarbonate spacers were then placed at the top, the container lids were put in place, and the containers were sealed closed. The polycarbonate spacers were used to ensure that all specimens remained completely submerged at all times. The filled containers were then placed on the shaker tables described previously, and the weight of the control specimens was periodically checked.

Static Tests

The majority of the static tests have been completed. All tests were run in displacement control at a loading rate of 0.025mm/s until failure. Typical load versus displacement plots are shown in Figure 6. Here, it is clear that the nonlinear point occurs well below the ultimate load. Figure 7 presents the ratio of the stress at the observed nonlinear point to the ultimate strength as a

function of condition, where the nonlinear point was obtained by visual means. In this and subsequent figures, the discrete symbols represent the average result from a given condition, and the error bars reflect the minimum and maximum values obtained. Interestingly, this figure shows that for the dry specimens at both temperatures, the nonlinear point occurs at a greater percentage of the ultimate strength in the damaged specimens than in the undamaged specimens, whereas for the wet specimens, the nonlinear point occurs at a lower percentage of ultimate strength in the damaged specimens as compared to the undamaged ones.

Figure 8 shows normalized stiffnesses from the static tests as a function of condition. Here, stiffness is defined as the slope of the load versus deflection plot, as obtained within the linear region, divided by the specimen's width (i.e., stiffness = [load/width]/deflection). All results in the figure are normalized by the average stiffness from the LTDU specimens, which was found to be 5.58 MPa. As would be expected, for the dry specimens, decreasing the temperature results in a small increase in stiffness. However, there is little effect of temperature on stiffness for the wet specimens. As would also be expected, for a given temperature and damage state, dry specimens are stiffer than sea water saturated specimens. Within the experimental scatter, only the RTD specimens show a clear effect of damage on stiffness.

As expected from the exploratory tests, all of the RTDU and RTDD static tests failed by core shear. However, it was found that both the static failure strength and the static failure *mode* for the other conditions were strongly influenced by environment. The test results are summarized in Figure 9. This figure presents the core shear stress and face sheet stress at failure as well as information on the failure mode. All stresses were determined based on the measured total thickness and computed face sheet thickness for that individual specimen. Similar to stiffness, for the dry specimens, strength increases with decreasing temperature, there is little effect of temperature on strength for the wet specimens, and for a given temperature and damage state, dry specimens have higher strength than sea water saturated specimens. Within the experimental scatter, there is no appreciable effect of the damage on ultimate strength.

Fatigue Tests

Fatigue testing is currently approximately 50% complete. Two of the three RTDU specimens have been cycled to failure, and all RTDD, LTDU and LTDD testing is complete. LTWU testing has just been initiated.

Initially, a series of exploratory tests were performed to choose the fatigue load levels. Our goal was to choose load levels for testing that would allow for quantitative comparisons across conditions and which would cause failures in the range of 50,000 to 1,000,000 cycles. Tests resulting in longer fatigue lives would not be feasible given the testing time that would be required. In our exploratory tests, load levels in the vicinity of the static nonlinear point were first considered. However, this resulted in extremely long fatigue lives. Subsequent exploratory tests indicated that peak load levels equal to 65% of the static ultimate strength at that condition would produce the desired result, and this load level was therefore chosen for testing. Thus, in view of the static strength results presented in Figure 8, the maximum load per unit width applied to the LTDU and LTDD specimens was 45,700 N/m, corresponding to a maximum core shear stress of 1.54 MPa and a maximum face sheet stress of 112.5 MPa. The LTWU, LTWD, RTDU and RTDD specimens are all being tested at a maximum load level of 36,000 N/m, which is 65% of their average ultimate strength, and 51% of the average ultimate strength of the LTDU and

LTDD specimens. The RTWU and RTWD specimens will likely also be tested at this same load level, although this decision has not yet been made.

All fatigue tests are being performed at a frequency of 4 Hz and with a minimum fatigue load that is 10% of the maximum value (i.e., R=0.1). These choices were based primarily on our literature review (described in the last interim report), and were felt to be most appropriate for subsequent comparison of our data to previous results.

All fatigue tests are being run in load control. Initial values of dynamic stiffness are being measured using a similar approach as for the static tests. Here, dynamic stiffness is defined as $(\Delta P/B)/\Delta\delta$, where ΔP is the difference between the maximum and minimum load, B is the specimen's width, and $\Delta\delta$ is the measured displacement that occurs over the cyclically applied ΔP. The initial dynamic stiffness is measured at approximately 500 cycles in order to allow the test to stabilize. Displacement triggers are used to provide periodic stops as well as to indicate specimen failure. For stops at which failure does not occur, dynamic stiffness is recorded approximately 500 cycles after the test is restarted. This allows the stiffness change to be recorded as a function of the number of loading cycles.

Figure 10 presents the normalized maximum load versus number of cycles to failure for those specimens already tested. The normalization is with respect to the ultimate load evidenced by the low temperature dry specimens. That is, as described above, these specimens were cycled at 65% of their ultimate strength. The room temperature dry specimens were also cycled at 65% of their static strength, which corresponds to 51% of the maximum strength of the LTD specimens. In contrast to the static strength results, for fatigue loading the presence of damage makes a significant difference. For both the LTD and RTD specimens, the life of the undamaged specimens was on the order of twice the life of the damaged specimens.

Figure 11 presents the same data as Figure 10, but here the maximum core and face sheet stress during cycling is plotted for each specimen based on that specimen's dimensions. Larger specimen-to-specimen variations in face sheet stress, as compared to core stress, are observed because face sheet stress is a much stronger function of face sheet thickness, which varied from panel to panel. All except two specimens failed by core shear; these two specimens are indicated in Figure 11, and failed by face sheet tension in the vicinity of the inner loading head. A typical core shear failure is shown in Figure 12.

Additional data, not presented in Figures 11 and 12, comes from two exploratory tests conducted at "-40°C." That is, these tests were begun at -40°C, but by the end the temperature had increased to the range of -21 to -25°C. The load for these tests was similar to that used for the RTDU and RTDD tests. One of these tests was stopped after 2.1M cycles with no failure, and the other specimen failed at 950,000 cycles. The data are not included in the plot due to the temperature fluctuation during the test. However, these results, and those in Figures 10 and 11, strongly support the assumption that fatigue life at a constant stress level increases with decreasing temperature.

Figure 13 presents typical plots of dynamic stiffness versus number of loading cycles for each type of specimen tested to-date, and Figure 14 presents the ratio of the final to the initial dynamic stiffness. All specimens show relatively little change in dynamic stiffness prior to failure.

Conclusions and Next Steps

The conclusions from the sandwich panel bending tests performed to-date are as follows:

- Environmental conditions that range from -20°C to room temperature and from dry to sea water saturated affect the bending strength and stiffness of composite sandwich structure; environment can also influence the *failure mode*. This has important implications for the accurate determination of material properties and points out the need for highly accurate failure models that are applicable across a range of usage environments.
- Dry sandwich structure tends to get stiffer and stronger as the temperature decreases from room temperature to -20°C. At a given temperature, sea water saturated structure tends to have lower strength and stiffness than dry structure.
- Impact damage can decrease static stiffness without having any significant effect on static strength.
- Static test results cannot be used to estimate fatigue behaviors. Impact damage showed little effect on static strength, but significantly decreased fatigue life at the conditions tested. Failure modes under static and fatigue loadings were also observed to differ under some environmental conditions.
- For dry, undamaged sandwich structure, fatigue life appears to increase with decreasing temperature.

Work in this area is continuing according to the following plan:

- Current emphasis is on completing the fatigue testing and reducing all data, at which time a comprehensive assessment of the effects of environment and damage will be made. If time and resources permit, we will also do a few additional fatigue tests so that we have data for specimens under the same loadings that will allow a direct comparison. That is, a few LTDU and LTDD specimens might be tested at a maximum fatigue load level of 36,000 N/m, which is the same stress level being used for the other conditions.
- A few of the static test results come from panels where only 4 good specimens were obtained. These tests appear to provide the most scatter. Additional tests will be done under the effected conditions to evaluate whether these results are valid.

Sandwich Debonding Test Assessment and Development

Overview

In the previous interim report, it was shown that nonlinear effects can have large effects on the perceived toughness as obtained by conventional modified split cantilever beam (MSCB) tests and tilted sandwich debond (TSD) tests oriented at 0°. These tests are shown schematically in Figures 15 and 16, respectively. It was also shown that the placement of the load cell in standard uniaxial load frames, i.e., whether the cell is mounted on the lower side or the upper side of the specimen, will have a tremendous effect on the perceived toughness from the MSCB test. As such, the MSCB is not expected to produce accurate toughness values, and the accuracy of the results from the TSD will depend upon the test geometry chosen. For this reason, a new test was investigated. This new test was referred to in the last interim report as the axially unconstrained bending test, and is shown in Figure 17. Subsequent to that time, however, we have found that this test was previously proposed. When initially introduced, it was referred to as the single cantilever beam (SCB) test [1]. However, these authors later referred to their test as the modified peel test [2,3] and used the term "SCB" to refer to a similar test that did not contain a linear bearing. This latter test is quite similar to the TSD test at 0°, except that the TSD is always shown as being supported along its entire base, whereas the SCB is shown as being clamped only at the uncracked end. Following the authors that introduced it, the test shown in Figure 17 will subsequently be referred to as the modified peel (MP) test. The data reduction method as originally introduced for both the MP and SCB tests was compliance calibration, identical to that used for composite double cantilever beam specimens. However, this approach, when applied to specimens with somewhat thin glass face sheets, will not provide accurate values of toughness. In our research, we have refined the data reduction process for the MP test, and believe that this test and our new data reduction method provide the most accurate means of determining face sheet debonding toughnesses in sandwich structures. This is based on extensive finite element and experimental investigations. The new work since our last interim report, and its associated implications, are described below.

Finite Element Analyses

As described in the last interim report, linear as well as geometrically nonlinear (NL) finite element (FE) analyses were performed of the MSCB, TSD and MP geometries. All FE models used 4-noded, two-dimensional plane stress elements. All elements in the vicinity of the crack tip were square with length close to $1/64^{th}$ of the face sheet thickness. Linear mesh refinement studies showed that this element size was sufficient to guarantee convergence in the total energy release rate. However, convergence studies with the NL models showed that the 4-noded elements evidenced extensive drawing and distortion at the crack tip, and the commonly used virtual crack closure technique did not produce converged results. For this reason, the J-integral approach was used to extract G. Comparisons of J with G as determined by a global energy balance indicated that this method gave highly accurate results and remained converged with increasing mesh density.

Extensive documentation of the MSCB and TSD results were presented in the last interim report and are not repeated here. Rather, in what follows, we focus on validation of the data reduction method of the MP test.

Data Reduction in the MP Test

As described in the last interim report, data reduction development focused on developing a modified version of the load only (LO) and load-displacement (LD) methods of data reduction originally developed by Williams et al. [4] for composite double cantilevered beam specimens. Considering that only one cracked leg of the cracked sandwich beam is displacing in the MP test, the expression for energy release rate, G, by the LO method for the MP test differs by a factor of 2 from the original expression by Williams et al and is given by

$$G_{LO} = \frac{6P_c^2(a+\chi h)^2 F}{B^2 h^3 E_{1f}} \tag{1}$$

where P_c is the critical load, a is the crack length, h is the face sheet thickness, B is the specimen's width, E_{1f} is the flexural modulus, and F corrects for the reduction in moment at the crack tip due to the effective shortening of the face sheet from large deflections as well as the possible presence of loading tabs. It is given by

$$F = 1 - \frac{6}{5}\left(\frac{\delta}{a}\right)^2 - \frac{3l_1\delta}{a^2} \tag{2}$$

In the above, δ is the deflection and l_1 is the distance from the center of the loading pin to the mid-plane of the delaminated face sheet. This expression was also modified from the original result obtained by Williams to account for the fact that only a single leg is displacing. The crack length correction factor, χ, in Eq. (1) accounts for crack tip rotations, shear deformations and the beam on an elastic foundation effect. It is found by a method similar to that proposed by Williams, et al. That is, both E_{1f} and χ are obtained from the slope and interception of the experimentally determined $(C/N)^{1/3}$ *vs a* curve following the approach described by Williams, but the following expression is used

$$\left(\frac{C}{N}\right)^{1/3} = \left(\frac{4}{Bh^3 E_{1f}}\right)^{1/3} (a+\chi h) \tag{3}$$

In the above, C is the compliance, which is defined as the slope of the deflection, δ, versus load, P, plot from the test at any given crack length. The parameter N is intended to correct for face sheet shortening due to large deflections and the possible stiffening from the loading tabs. It is given by

$$N = 1 - \left(\frac{l_2}{a}\right)^3 - \frac{9}{4}\frac{\delta l_1}{a^2}\left[1 - \left(\frac{l_2}{a}\right)^2\right] - \frac{36}{35}\left(\frac{\delta}{a}\right)^2 \tag{4}$$

where l_2 is half of the height of the end tab. If a hinge is used to introduce the load, then $l_2 = 0$. Equation (4) is also a modified version of the expression given by Williams.

When computing G by the LD method, the displacement of only a single leg enters into the expression. Since this displacement differs by a factor of 2 from the case where both legs contain cracks (or a single DCB), the original expression by Williams is recovered, i.e.,

$$G_{LD} = \frac{3P_c\delta_c}{2B(a+\chi h)}\frac{F}{N} \tag{5}$$

The key practical issue that arises when implementing the above approach lies in the determination of E_{1f} and χ. As described above, to obtain these values, one first determines the compliance of the MP specimen at each crack length, a. However, since there will be some nonlinearity in the load versus deflection plots, one will obtain different values of compliance, C, depending on the load and displacement level used for the linear regression analysis used to obtain C. In theory, the parameter N is intended to account for this, but in practice, different values of E_{1f} and χ are obtained over different ranges of curve-fit. This effect is much more pronounced in the MP than in typical DCB testing because of the relatively larger deflections that occur, particularly with glass-reinforced face sheets at large crack lengths.

In order to address the above, a number of MP geometries were modeled and the energy release rate (ERR) was obtained through application of the J integral at a variety of crack lengths using NL FE analysis. Next, the load versus deflection results generated by the NL FE model were used to evaluate the LO and LD data reduction techniques using various criteria for determining compliance. The resulting value of ERR was then compared to J to assess the accuracy of the various methods. Methods considered for fitting the compliance included constant load, constant displacement, constant ERR, and various compliance offsets. We began by assuming loading blocks would be used (as shown in Figure 16), but found that a hinged loading tab provided much higher accuracy. Thus, in what follows, all results assume a hinged loading tab.

Of the methods evaluated, the most accurate approach, as well as the one that would be most easily implementable in actual testing, was a "95% compliance offset" method. Here, the compliance from the initial portion of the δ versus P curve is computed and used to find the intersection of the loading line with the zero load point; in practice, this accounts for any initial nonlinear portion of the curve that is possibly associated with take-up of free play in the system. Next, a line of slope 0.95C (corresponding to a 5.2% stiffness increase) is projected from this intersection point until it intersects with the δ versus P curve. That is, the NL FE analysis predicts that the slope of the loading line will increase due to the stiffening effect associated with the load-arm shortening. The portion of the δ versus P curve above any initial nonlinearities and up to this intersection point is used to compute C/N for use in Eq. (3). If there is insufficient stiffening for the 0.95C and the loading lines to intersect, then the entire loading line (excluding any initial NL region) is used for the determination of C/N.

To illustrate, Tables 1 and 2 present material and geometric properties used in the NL FE analyses. These properties were used to analyze specimens with crack lengths from 25.4 to 76.2mm in 12.7mm increments. Two cases were considered: one with the critical ERR, G_c, in the vicinity of 350 J/m^2, and the second with $G_c \approx 1100$ J/m^2. Table 3 presents the error in the LO and LD methods of data reduction (i.e., in comparison to the results by J-integral) for glass fabric

and graphite fabric face sheets of 6 and 12 ply thicknesses with the two assumed values of G_c. Here, the mean and minimum errors refer to the average and minimum values, respectively, from all crack lengths studied. The table also presents the average and minimum values of F, Eq. (2), which are defined in a similar manner. The importance of these values will be discussed subsequently.

In general, Table 3 shows that ERRs obtained by LD method are slightly more accurate than by the LO method. Note that ERRs obtained by both methods are fairly accurate for graphite face sheets for all thicknesses and values of G_c. However, for glass face sheets in a material with G_c = 1100 J/m^2, the method is not capable of extracting G_c with extremely high accuracy. Thus, in this type of a situation, testing specimens with 12-ply thick face sheets would be recommended.

Table 1. Face sheet, core and adhesive properties.

Parameter	Glass fabric face sheet	Graphite fabric face sheet	Core	Adhesive
Modulus (GPa)	10.8	47.5	0.065	2.6
Poisson's ratio	0.11	0.04	0.337	0.3
Thickness: 6 ply model (mm)	1.45	1.45	25.4	0.254
Thickness: 12 ply model (mm)	2.51	2.51	25.4	0.254

Table 2. Loading hinge properties.

Length (mm)	12.7	Modulus (GPa)	200.0
Height (mm)	1.52	Poisson's ratio	0.29
Pin diameter (mm)	3.18		

Table 3. Errors from LO and LD data reduction methods.

Method	Face Sheet Thickness	G_c (J/m^2)	Glass face sheets				Graphite face sheets			
			Mean error (%)	Max error (%)	F		Mean error (%)	Max error (%)	F	
					Avg	Min			Avg	Min
LO	6-ply	350	-2.84	-3.40	0.812	0.756	-0.21	-0.97	0.912	0.885
LO	6-ply	1100	-9.81	-11.47	0.581	0.432	-3.94	-5.70	0.800	0.703
LO	12-ply	350	-1.50	-2.12	0.934	0.914	-1.09	-1.82	0.969	0.962
LO	12-ply	1100	-5.83	-6.57	0.809	0.772	-2.89	-3.90	0.916	0.899
LD	6-ply	350	-2.56	-2.95	0.812	0.756	-0.73	-1.47	0.912	0.885
LD	6-ply	1100	-8.00	-10.69	0.581	0.432	-2.62	-3.97	0.800	0.703
LD	12-ply	350	-1.79	-2.15	0.934	0.914	-1.21	-1.78	0.969	0.962
LD	12-ply	1100	-5.20	-5.38	0.809	0.772	-2.72	-3.45	0.916	0.899

The above discussion brings up the interesting problem that one must know – without the benefit on NLFE – what the accuracy of the method is. This information would be critical to deciding whether or not G_c could be extracted accurately from sandwich structure of a given material and face sheet thickness. Alternatively, one could think of this type of information as being used to design appropriate tests. To address this, various "cut-off" criteria were evaluated. Methods considered included expressions based on F, N, and various measures of nondimensionalized displacement. Once a candidate approach was found, additional geometries were then analyzed to make sure that the chosen method would be widely applicable. The most promising method, and one that could also be easily implemented in practice, was based on the parameter F. This is illustrated in Figure 18. Figure 18a presents the error in the ERR as predicted by the LD method for all cases considered. Similar results for the LO method are presented in Figure 18b.

In practical applications, if one excludes results from tests where $F<0.73$ due to potential data reduction errors, then the worst-case error based on all of our simulations would be -5.4% if the LD method is used and -6.8% if the LO method is used. Referring once again to Table 3, it was found that F is less than 0.73 by both methods for all crack lengths for the specimens with 6 ply glass fabric face sheets and a toughness of 1100 J/m^2. Thus, if one were to perform an experiment on specimens of this type, the first test would yield values of F in the range of 0.58. Based on the cut-off criterion, this would provide the feedback that this is not an acceptable test geometry. One would also expect to see reasonably large nonlinearities in the load versus deflection plots. For sandwich structure with 6 ply graphite fabric face sheets and a toughness of 1100 J/m^2, the NL FE results indicate that F will be greater than 0.73 for crack lengths less than approximately 74mm. Thus, if one was performing tests of this geometry, the cut-off criterion provides a means to know up to what crack length the values of G_c are expected to be reliable.

Experiments

A series of experiments were performed on sandwich panel specimens to validate the previous results. All specimens used 25.4mm thick DIAB H100 core, BGF 7532 plain weave glass fabric and Dow Chemical's Derakane 411-350 vinyl ester resin. 300mm long x 225mm wide panels were fabricated with 6, 12 and 18 ply thick face sheets. At one end of the panel, a 75mm long, 13μm thick teflon insert was placed at the interface between the core and one of the face sheets to serve as a starter crack. The 6 ply face sheets used a $[0/90/0]_s$ stacking sequence, the 12 ply used a $[0/90/0/0/90/0]_s$ sequence, and the 18 ply layup was $[0/90/0/90/0/90/0/90/0]_s$. Here, 0° is defined to be the warp direction. Following manufacture, panels were cut into 25mm wide test specimens using a band saw.

Figures 19a and 19b present load versus deflection plots from tests of MSCB specimens with 6 and 12 ply face sheets, respectively. A great deal of nonlinearity is present in the 6 ply specimen results, and these results show that the measured load can in fact be compressive for this test. Figures 20 and 21 present toughness results. Figure 20 presents results by the modified beam theory (MBT) method of data reduction, and Figure 21 presents results by the compliance calibration (CC) method. These were the two of the three methods studied in Ref. [5], in which it was concluded that either method could be used with essentially equal accuracy. The results in Figures 20 and 21 are quite similar, and results by the third method recommended in Ref. [5], the

modified compliance calibration method, were also computed and did not differ appreciably from those presented in the two figures.

All specimens tested in Figures 20 and 21 had initial crack lengths of approximately 25mm. Thus, the results that are presented consist of G_c versus a, or resistance (R) curves, for two specimens with 6 ply thick face sheets and two specimens with 12 ply thick face sheets. The key result from these figures is the strong dependence of the perceived toughness on the test geometry. That is, dramatically different results for fracture initiation are obtained from the 6 ply versus the 12 ply specimens. The two specimen thicknesses also display dramatically different resistance curves. The difference is so large because the problems with the MSCB lie not only in the effect of geometric nonlinearities, but also in the fact that conventional test frames, with a set-up as shown in Figure 15, measure the wrong load, i.e., as demonstrated in the last interim report, the load at the load cell does not equal the load at the actuator. This is also why a compressive load is obtained in Figure 19a. Thus, the MSCB test is not suggested for general use.

The TSD test was also used to obtain G_c from 12 and 18 ply specimens. Toughness values from the TSD specimens were higher than those by the MSCB. However, these tests were performed with long extension rods between the actuator and the lower portion of the fixture and between the load cell and the upper portion of the fixture. Our FE results indicate that this can significantly influence the results, as it makes the in-plane compliance of the system fairly large. This decreases the in-plane force and therefore the nonlinearity. For this reason, the 12 and 18 ply TSD tests are being repeated without extension rods.

Figure 22 presents load versus deflection plots from 12 ply MP specimens. It can be observed that the curves are fairly linear. Figure 23 presents the R-curves from all the MP tests performed. Good agreement among specimens is obtained. In contrast to the MSCB test, the R-curve is relatively flat.

Conclusions and Next Steps

The conclusions from the sandwich debonding test assessment and development study are as follows:

- The problems with the MSCB test described in the last interim report have been demonstrated experimentally. Experiments on the TSD test show the expected behaviors, but additional tests with a stiff system need to be done to provide quantitative comparisons to FE results.
- Experiments using the MP test have behaved essentially as expected. It appears that relatively simple data reduction methods can be used with the MP test to obtain highly accurate values of toughness for a wide range of practical test conditions.

Work in this area is continuing according to the following plan:

- Complete a few additional tests to complete the study of the MP test.

- Prepare a publication on the MP test and data reduction method for publication in the upcoming special volume of Strain: "Major Accomplishments in Composite Materials and Sandwich Structures – An Anthology of ONR Sponsored Research"
- Use the new MP test and associated data reduction method to perform sandwich debonding experiments as a function of moisture and temperature (specimens for this have already been manufactured, and sea water conditioning of approximately 50% of these specimens is nearing completion).

Plans, Staffing and Timeline

Figure 24 presents a Gantt chart for the schedule-of-work through project completion. It can be observed that the pace of the work is continuing to proceed at a satisfactory level. We are a bit behind the planned schedule on the immersion study, but ahead of schedule on the fatigue study. Budgetary spending on the project is also proceeding essentially as expected. In addition to the PI, the project is currently supporting one full-time graduate research assistant and a post-doctoral researcher at approximately 30% effort. This staffing situation is expected to continue through the project's end-date.

Conclusions

Significant research progress has been made during the past six months in the three research focus areas: (1) immersion studies of core and sandwich laminates, (2) effects of environment on impact damage and fatigue response, and (3) debonding test development and toughness assessments. Further, this research program is on track for completing all of its stated objectives during the following period of work, which will be the final six-month period of this study's t

References

1. Cantwell W.J. and Davies, P., "A Test Technique for Assessing Core-Skin Adhesion in Composite Sandwich Structures," *Journal of Materials Science Letters*, Vol. 13, 1994, pp. 203-205
2. Cantwell W.J. and Davies, P., "A Study of Skin Core Adhesion in Glass Fiber Reinforced Sandwich Materials," *Applied Composite Materials*, Vol. 3, 1996, pp. 407-420
3. Cantwell W.J., Broster, G. and Davies, P., "The Influence of Water Immersion on Skin-Core Debonding in GFRP-Balsa Sandwich Structures," *Journal of Reinforced Plastics and Composites*, Vol. 15, No. 11, 1996, pp. 1161-1172.
4. Hashemi, S., Kinloch, A.J. and Williams, J.G., 1990, "The Analysis of Interlaminar Fracture in Uniaxial Fibre-Polymer Composites," *Proc. R. Soc. London*, Vol. 427, pp. 173-199.
5. Shivakumar, K., Chen, H. and Smith, S.A., "An Evaluation of Data Reduction Methods for Opening Mode Fracture Toughness of Sandwich Panels," *Journal of Sandwich Structures and Materials,* Vol. 7, No. 1, 2005, pp. 77-90.

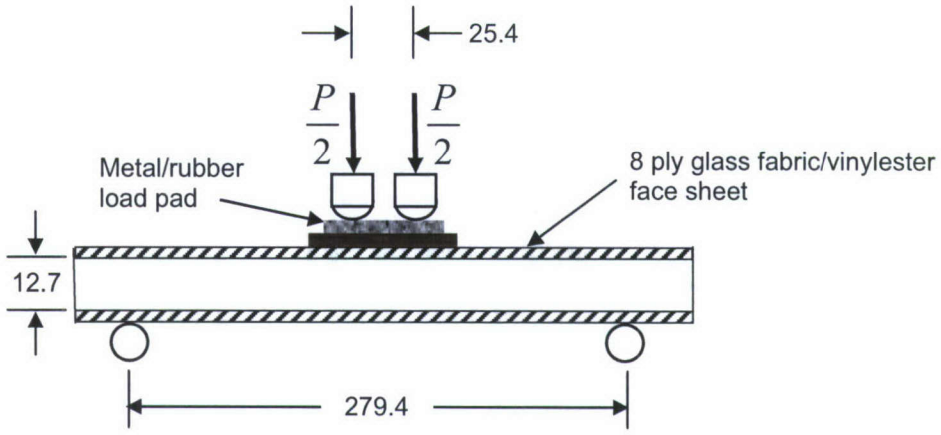

Figure 1. Schematic of bending test geometry (all dimensions are in mm).

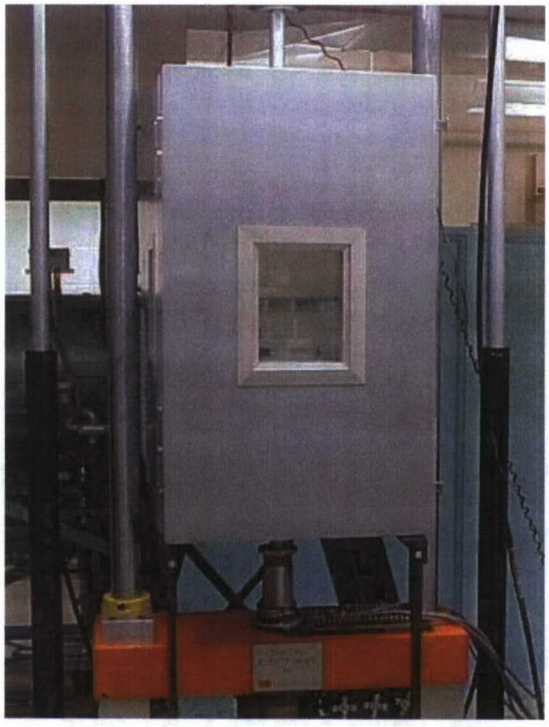

Figure 2. SU-CML low temperature chamber.

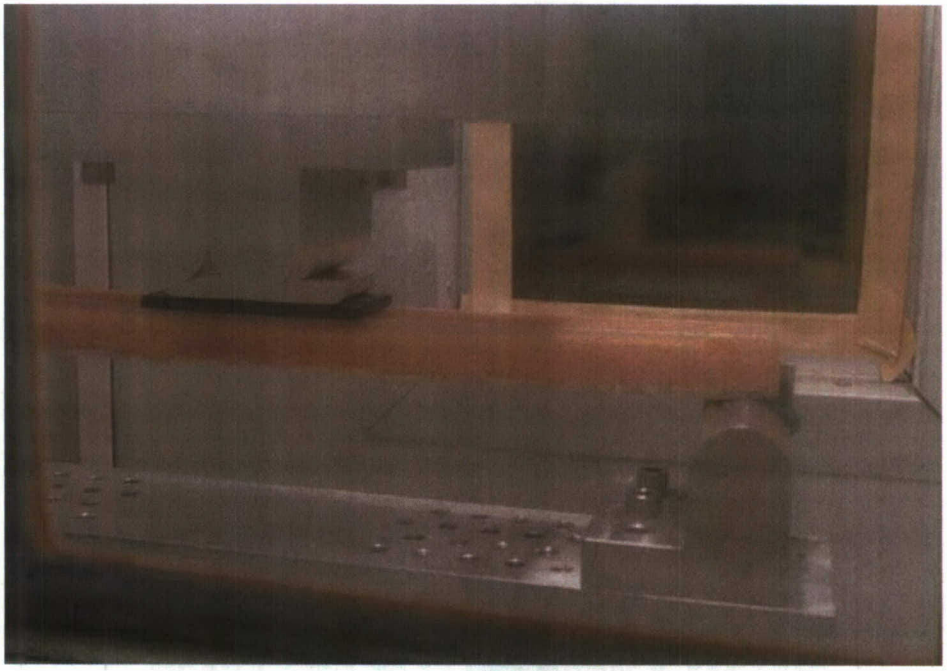

Figure 3. Close-up in region of load pad.

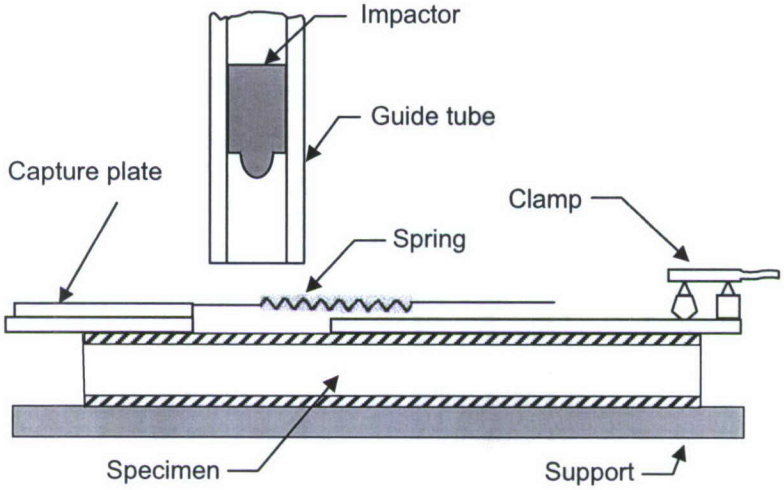

Figure 4. Schematic of impact fixture.

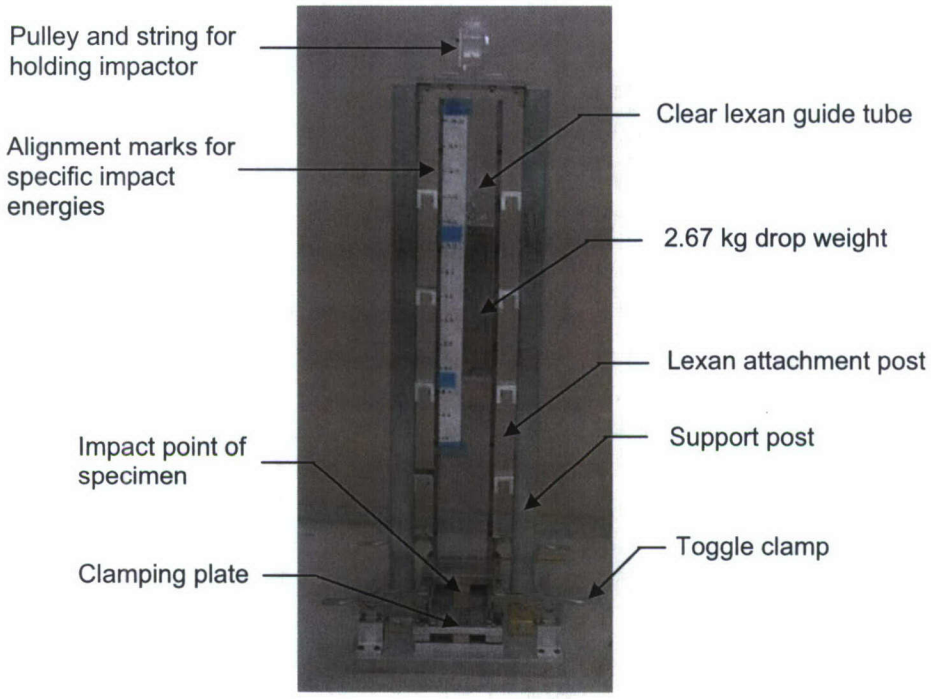

Figure 5. Photograph of impact fixture.

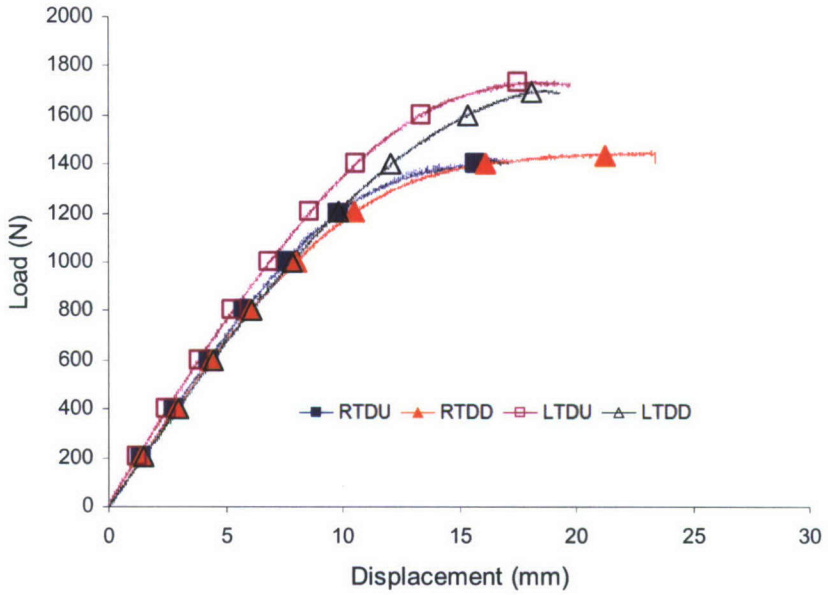

(a)

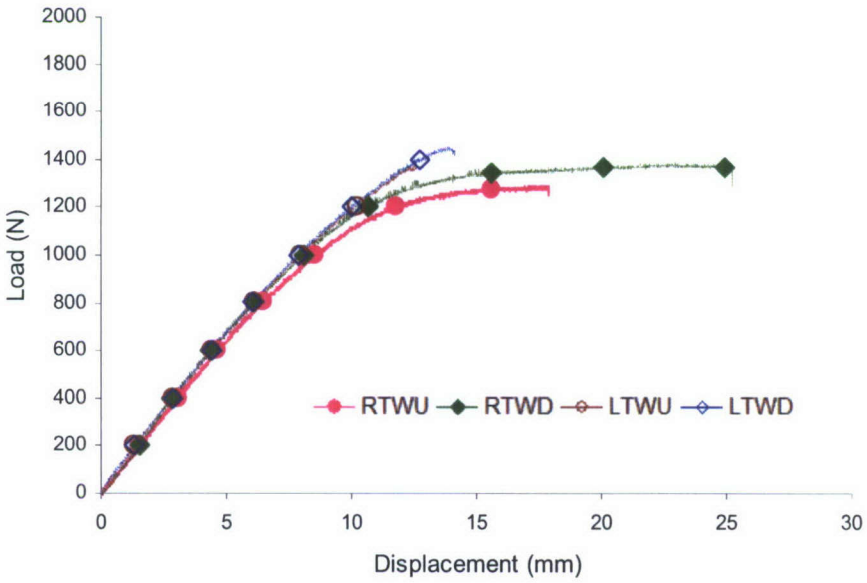

(b)

Figure 6. Typical load versus displacement plots.

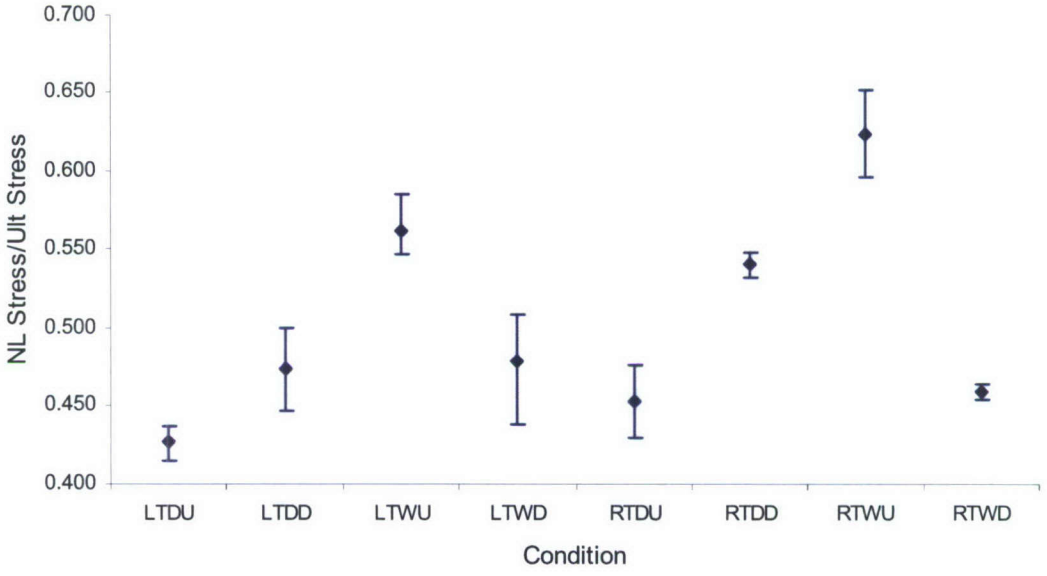

Figure 7. Ratio of nonlinear point stress to ultimate strength as a function of condition.

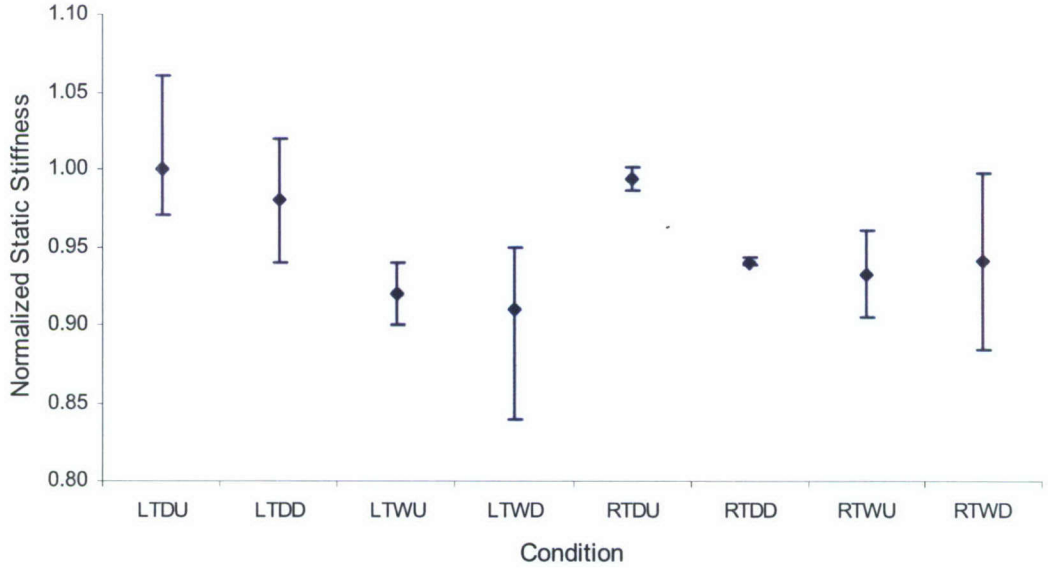

Figure 8. Normalized static stiffness versus condition.

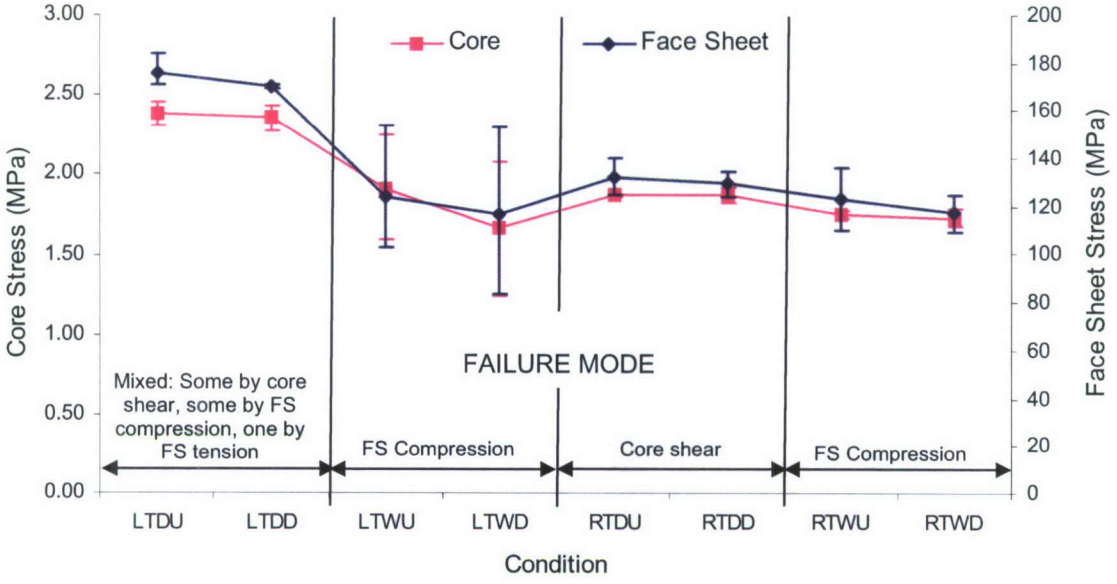

Figure 9. Static test results.

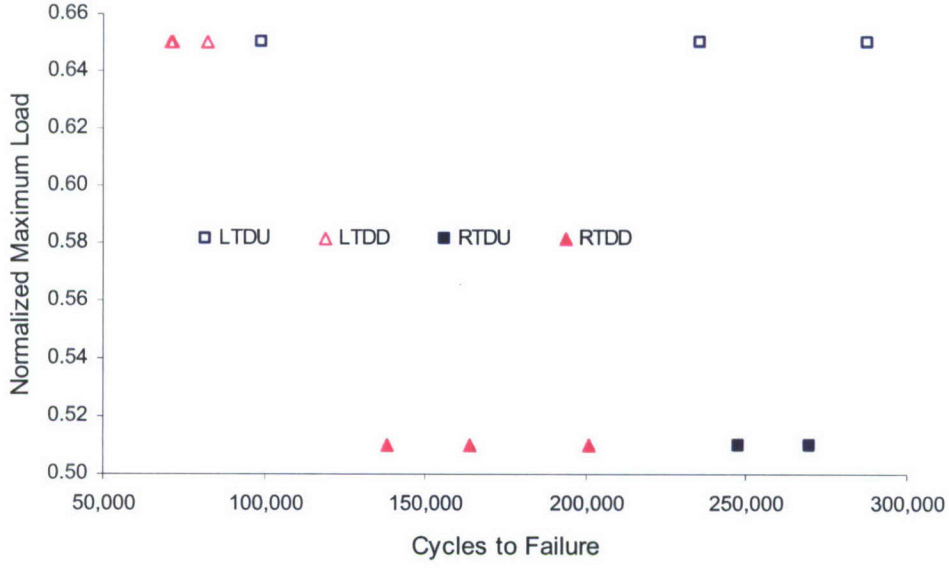

Figure 10. Normalized maximum load versus cycles to failure.

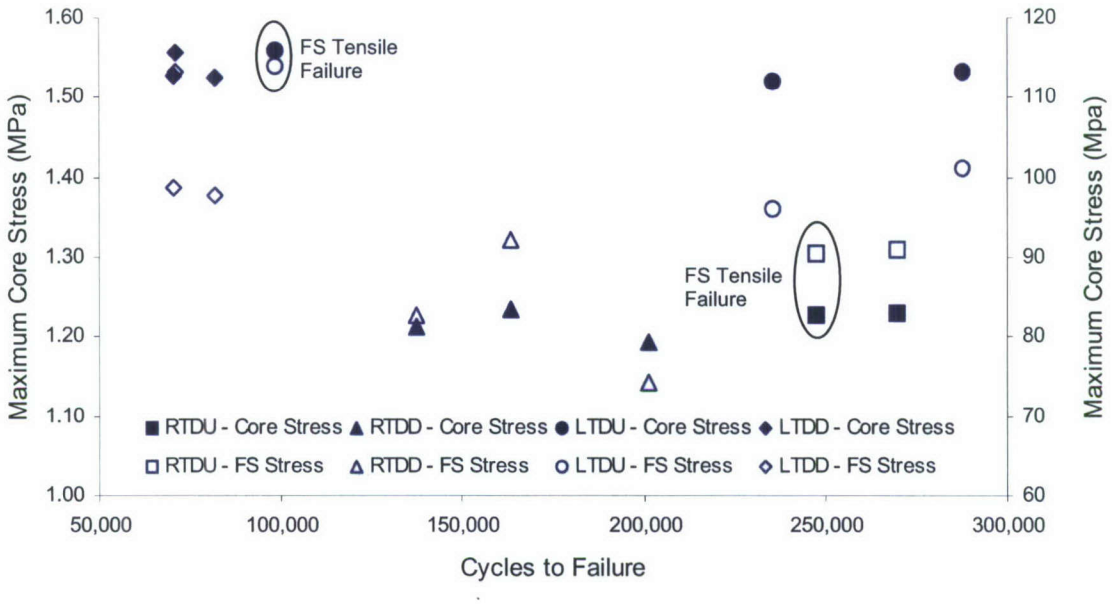

Figure 11. Core and face sheet stress versus cycles to failure.

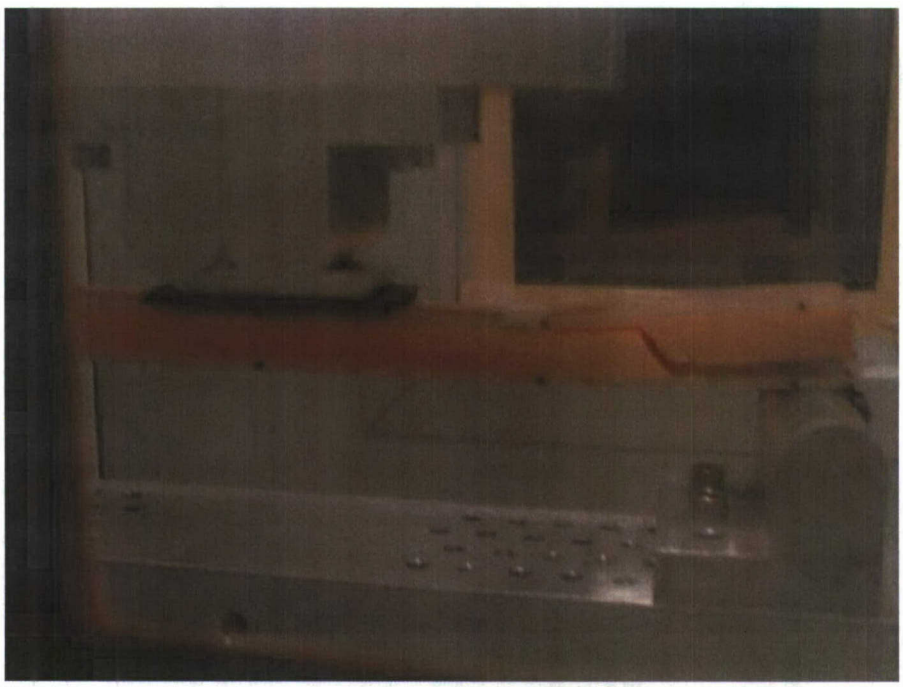

Figure 12. Typical core shear fatigue failure.

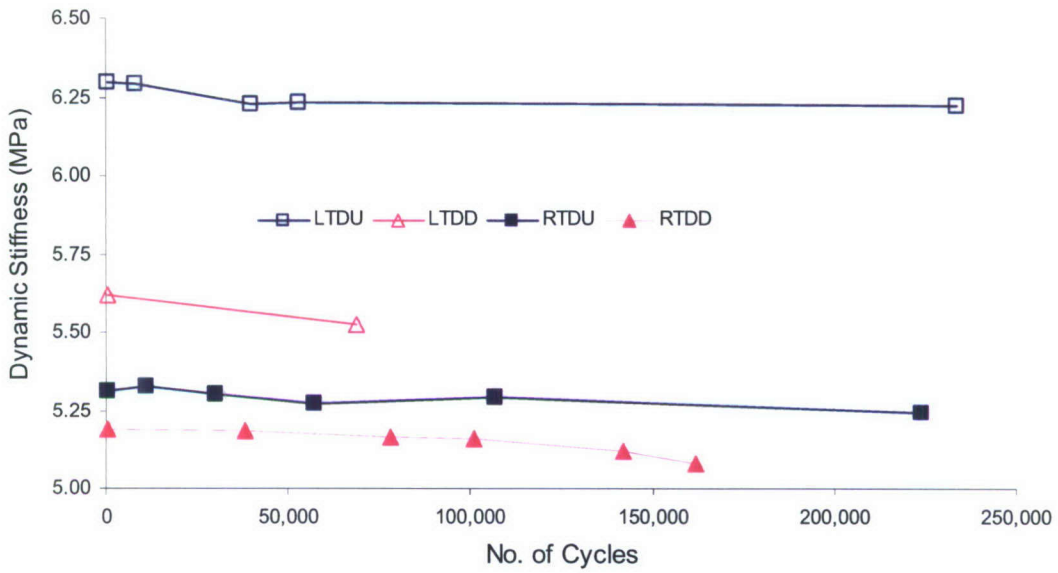

Figure 13. Typical plots of dynamic stiffness versus number of cycles.

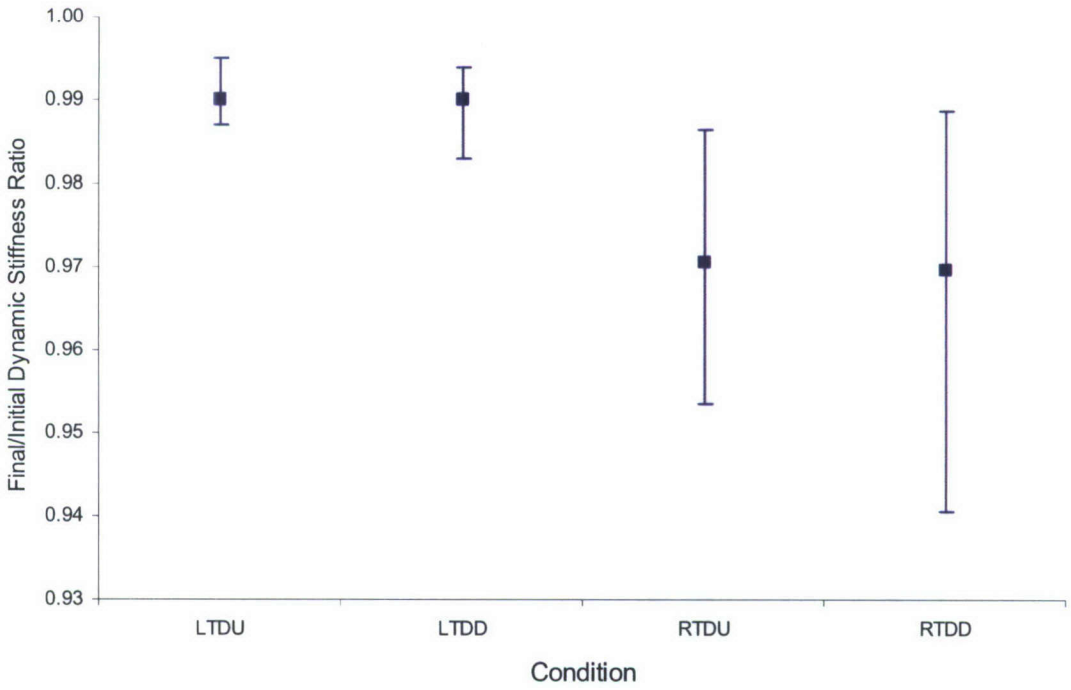

Figure 14. Ratio of final to initial dynamic stiffness as a function of test conditions.

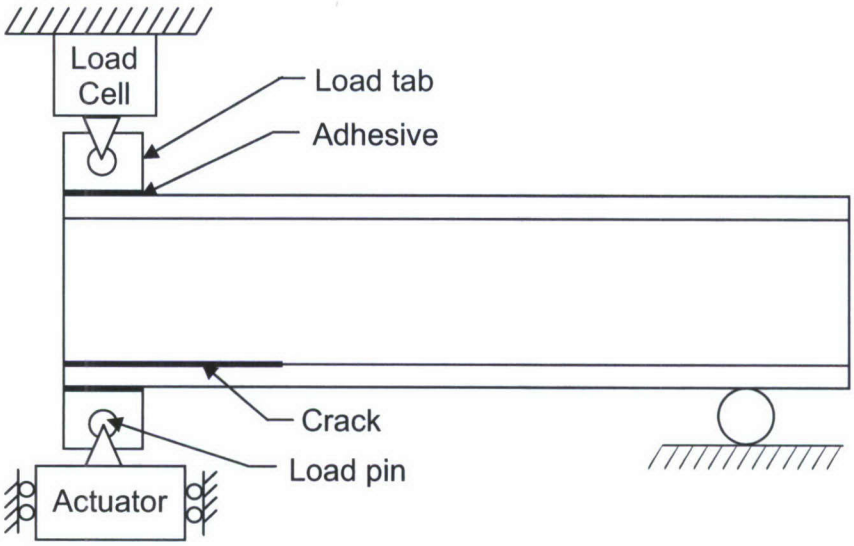

Figure 15. Schematic of the modified split cantilever beam test.

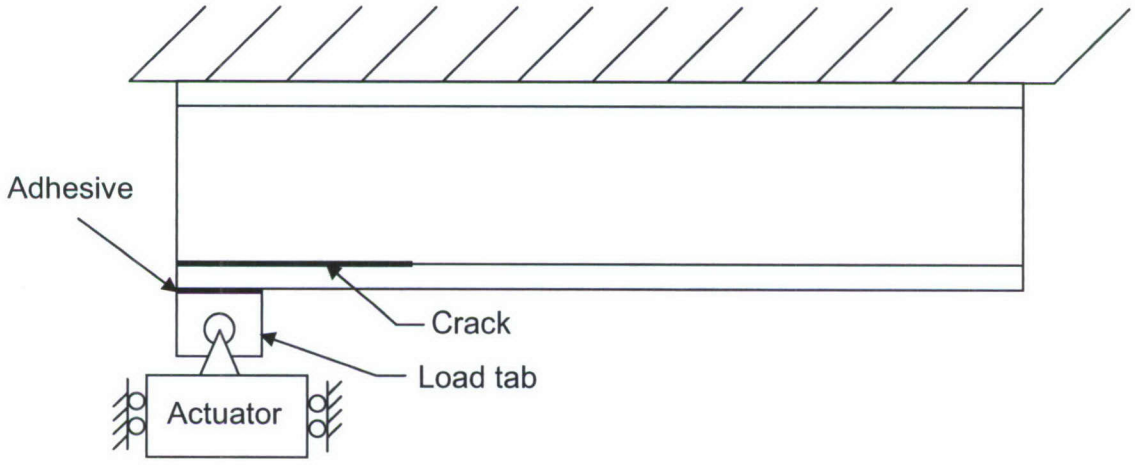

Figure 16. The tilted sandwich debond test at an angle of 0°.

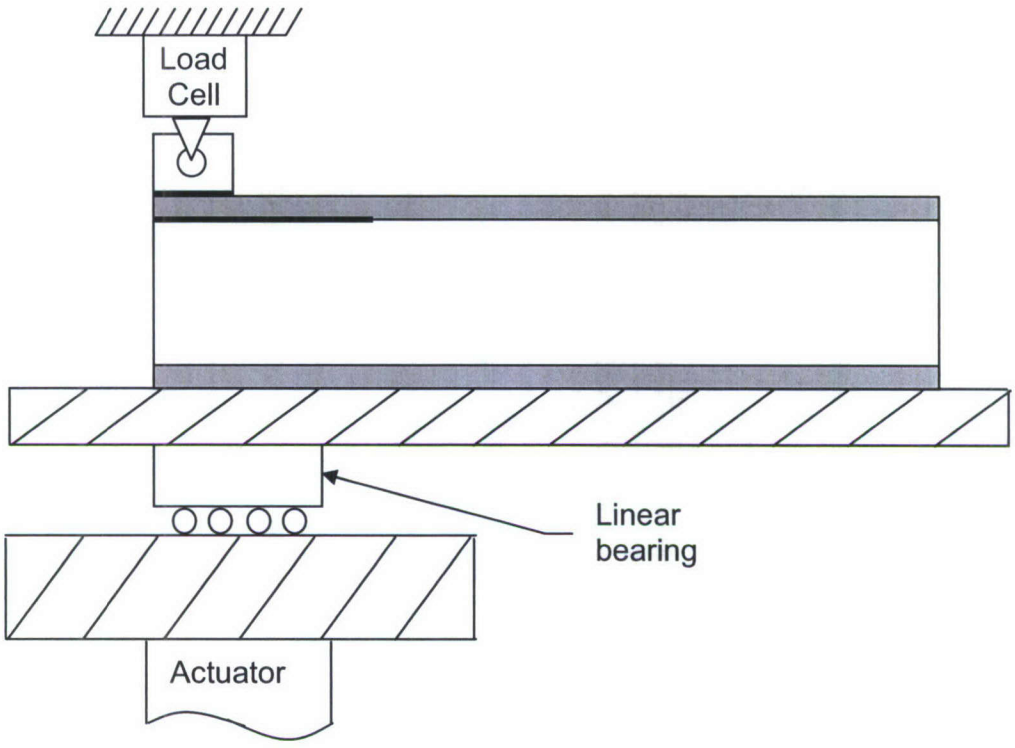

Figure 17. Schematic of the modified peel test.

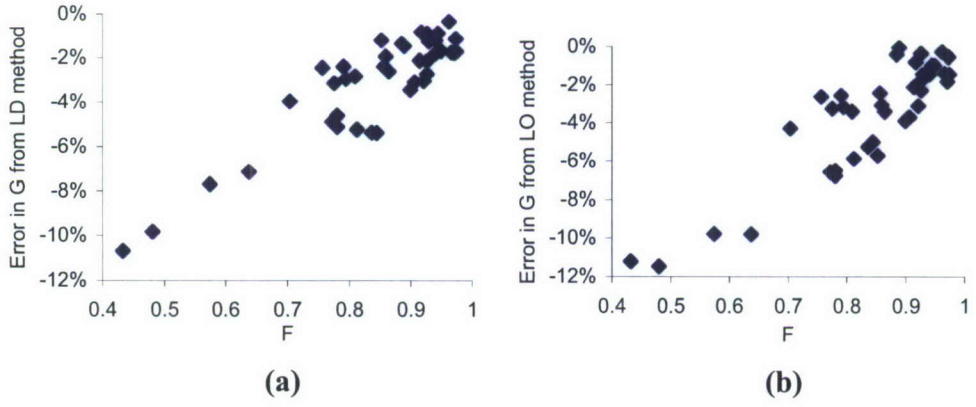

(a) **(b)**

Figure 18. Errors in ERR by (a) LD and (b) LO method in comparison to J by FE analysis.

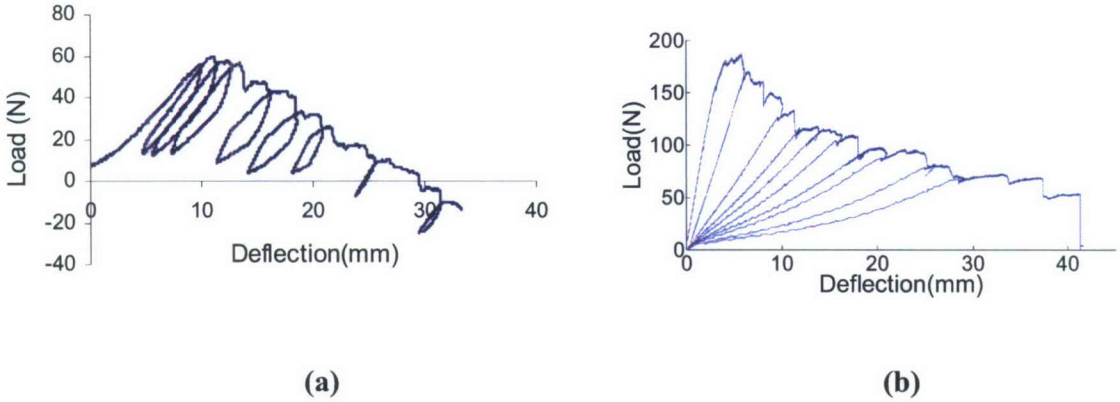

Figure 19. Load versus deflection plot from MCSB test of specimen with (a) 6 ply and (b) 12 ply face sheets.

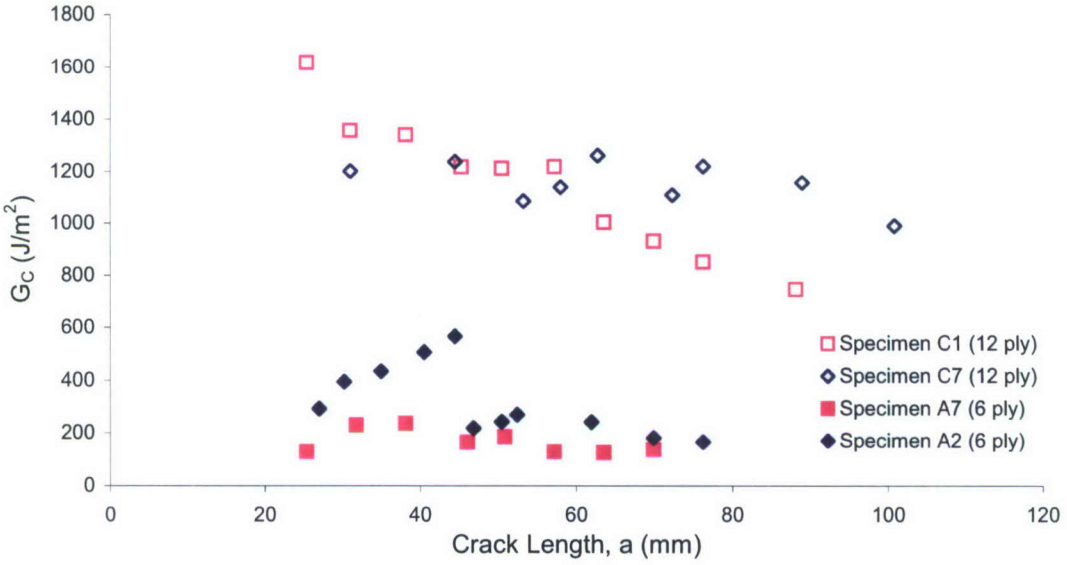

Figure 20. Toughness from MCSB by MBT method.

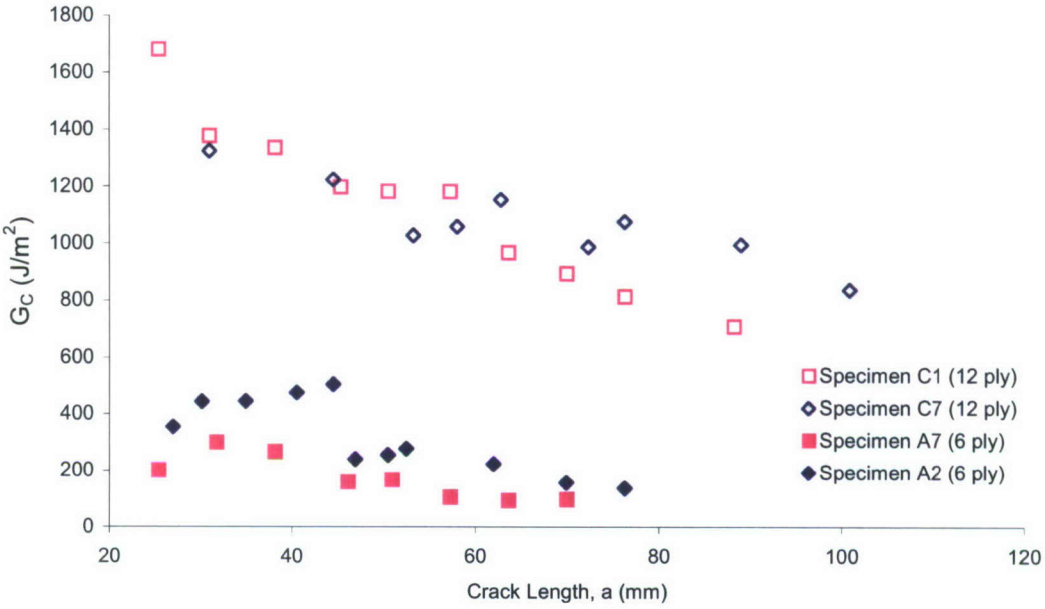

Figure 21. Toughness from MCSB by CC method.

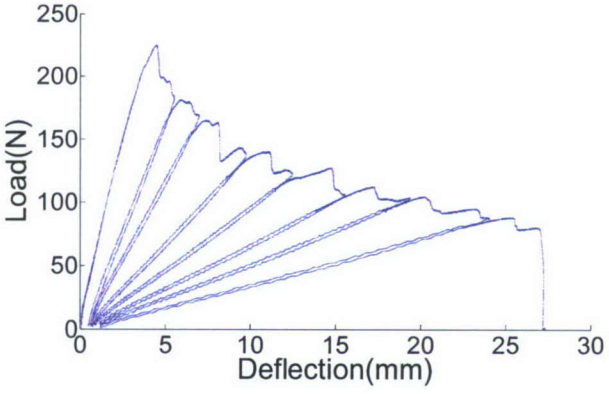

Figure 22. Load versus deflection plots from MP test of specimen with 12 ply face sheets.

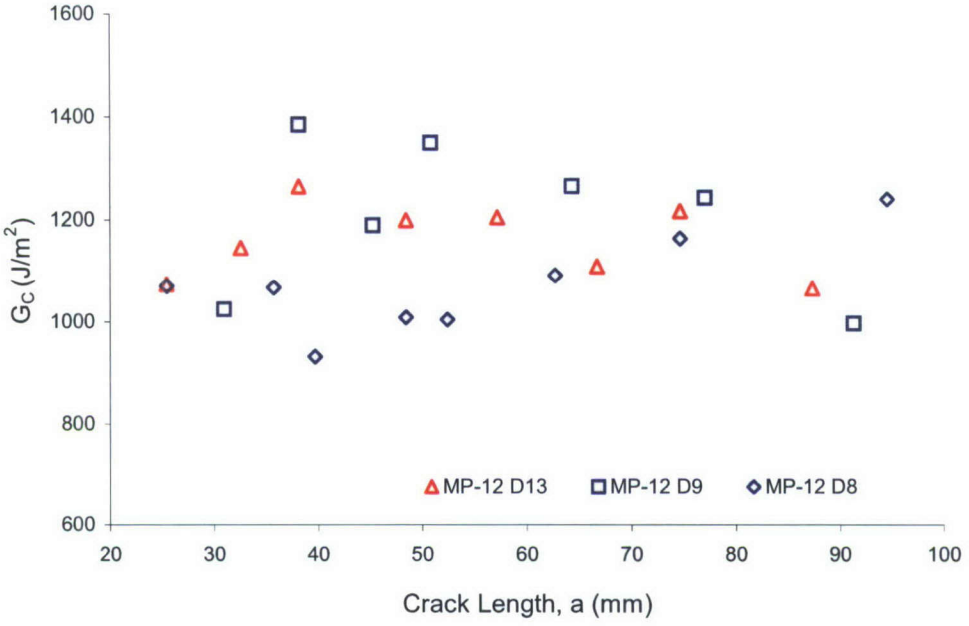

Figure 23. Resistance curves from MP specimens.

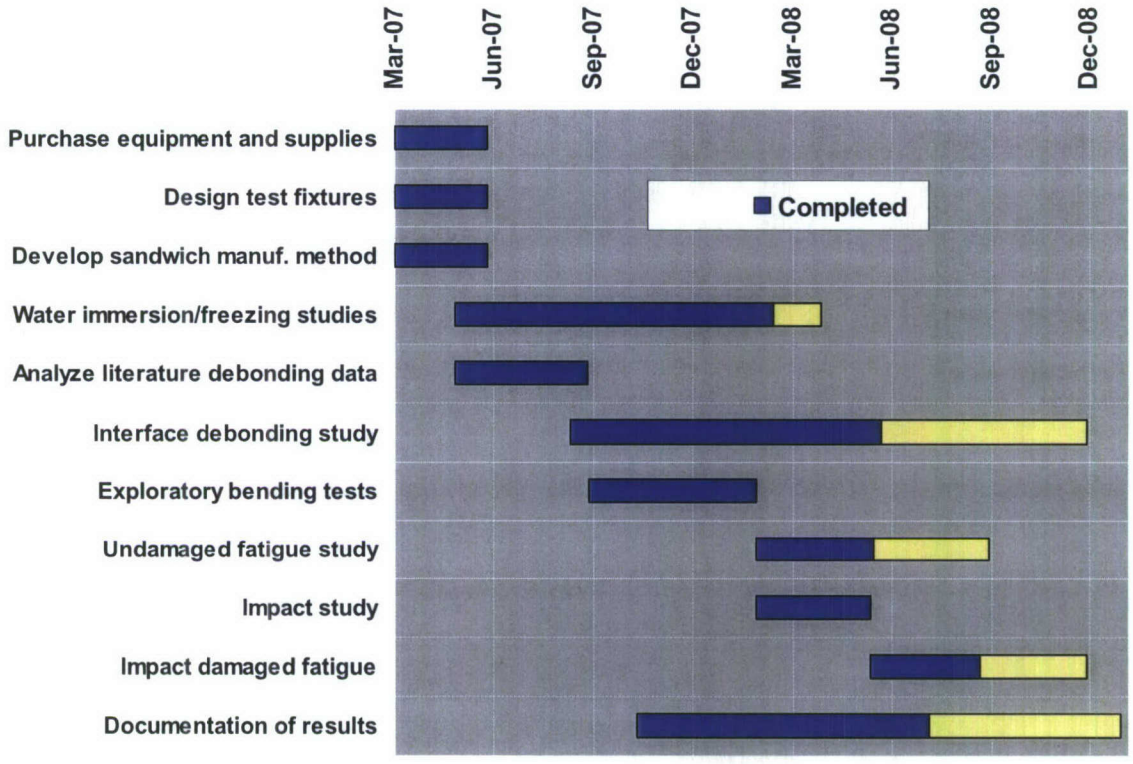

Figure 24. Schedule-of-work through project completion.